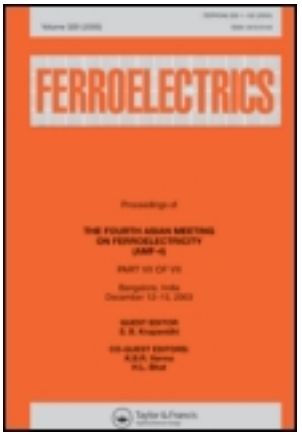

Ferroelectrics

Publication details, including instructions for authors and subscription information:
http://www.tandfonline.com/loi/gfer20

Wet Chemical Etching Process of BST Thin Films for Pyroelectric Infrared Detectors

Tianjin Zhang [a], He Huang [a] & Ren Chen [a]

[a] School of Materials Science and Engineering, Hubei University, Wuhan, 430062, Hubei, China

Available online: 20 Jan 2011

To cite this article: Tianjin Zhang, He Huang & Ren Chen (2010): Wet Chemical Etching Process of BST Thin Films for Pyroelectric Infrared Detectors, Ferroelectrics, 410:1, 137-144

To link to this article: http://dx.doi.org/10.1080/00150193.2010.492740

Ferroelectrics, 410:137–144, 2011

ISSN: 0015-0193 print / 1563-5112 online
DOI: 10.1080/00150193.2010.492740

Taylor & Francis
Taylor & Francis Group

Wet Chemical Etching Process of BST Thin Films for Pyroelectric Infrared Detectors

TIANJIN ZHANG,* HE HUANG, AND REN CHEN

School of Materials Science and Engineering, Hubei University, Wuhan 430062, Hubei, China

$Ba_{0.8}Sr_{0.2}TiO_3$ (BST) thin films were prepared on Pt/Ti/SiO_2/Si substrates by sol-gel processing. The BST thin films were patterned by wet chemical etching and the electrodes were shaped by lift-off technique. An improved etchant with the volume ratio of $HF:HNO_3:H_2O_2:H_2O = 1:25:50:20$ was developed for BST films etching. SEM graph shows that the unetched BST thin film is dense, crack-free and pore-free. EDS analyses indicate that Ba, Sr and Ti elements of etched areas are removed completely. XRD and AFM results show that the etchant-induced damage of the etched BST films could be partially recovered by post-annealing treatment.

Keywords Barium strontium titanate(BST); sol-gel processing; lift-off technique; wet chemical etching; etchant

Introduction

Ferroelectric materials have been extensively studied for the use in future generation integrated dynamic access memories (DRAM) [1] and uncooled infrared focal plane arrays (UFPA) [2]. Among numerous ferroelectrics, (Ba,Sr)TiO_3 (BST) thin films are known as one of the leading candidates of ferroelectric materials for such applications owing to its excellent properties including high dielectric constant, low dielectric loss, small leakage current and composition-dependent curie temperature [3]. In order to realize highly integrated silicon-based microelectronic devices involving BST films, the etching techniques of BST films should be developed.

Etching processes, such as inductively coupled plasma [4], reaction ion etching [5], ion beam etching [6] and wet chemical etching [7] have been used in producing of the BST film devices. Although dry etch processes can achieve an anisotropic etch profile. The difficulties are that there are plasma induced-damage and specialized equipment is needed [8, 9, 10]. Compared with dry etch, wet chemical etching with higher selectivity is economical and efficient to most semiconductor device fabrication.

In the past, various etchants such as BHF and KOH based chemicals were used to etch BST thin films [11]. However, they can react with photoresist and some residues are left. So it is necessary to find new etchant for BST films. In this work, we developed a suitable etchant by mixing HF, HNO_3, H_2O_2 and H_2O. The wet etching process was discussed in detail and the etching characteristics were also studied.

Received August 23, 2009; in final form October 19, 2009.
*Corresponding author. E-mail: tj65zhang@yahoo.com.cn

2. Experimental Details

N-type (100) silicon wafer with a resistivity of 2∼4 Ω·m was used as the substrate material. A SiO_2 layer with a thickness of 500 nm was grown by thermal oxidation. A thin Ti layer was deposited to promote adhesion of Pt to SiO_2 layer. Pt/Ti bottom electrode films, Ni/Cr absorption layer and Au top electrode films were deposited by direct current sputtering. They were all patterned by lift-off technique.

The precursor solution of BST thin films was prepared by acetic acid based sol-gel route. Barium acetate, strontium acetate and tetrabutyl titanate were used as starting materials. Glacial acetic acid was used as stabilizer agent, and 2-methoxyethanol was used as solvent. After stoichiometrically dissolved, the concentration of the $Ba_{0.8}Sr_{0.2}TiO_3$ sol was 0.2 mol/L.

The BST thin films were spin-coated on $Pt/Ti/SiO_2/Si$ substrates at 3000 rpm for 30 s and then kept at 450°C for 30 min to remove organic materials. A suitable heating process was determined to prevent the BST films from cracking. This procedure was repeated several times to obtain the final thickness of 500 nm. The pre-baked films were annealed at 700°C for 1 h in a tube furnace to form the perovskite phase.

The BST films were patterned by photolithography in several procedures. Firstly, coat positive photoresist (type AZ5214E) onto the thin films. Secondly, transfer the pattern from the mask to photoresist by mask aligners and exposure systems (ABM, Mask Aligners and Exposure Systems). Thirdly, remove the exposed photoresist by developer solution. Then post-bake the films on a hot plate under 115°C for 30 min. At last, etch the thin films by various etchants. The photoresist on the finished samples was stripped off by acetone.

The BST films crystal structure was analysed by X-ray diffraction (XRD, D/MAX-IIIC) with Cu K_α radiation ($\lambda = 1.5406$Å) at 35 KV, 25 mA and a scanning speed of 10 deg/min. The surface morphology of the films was analysed using an atomic force microscopy (AFM, Shimadzu SPM-9500J3). The microstructure of the films was observed by scanning electron microscopy (NOVA Nano SEM400). The film surface chemical compositions were assessed by energy dispersive spectroscopy (EDS). The etching rate was determined using a profilometer (Taylor Hobson Form, Taylor surf Series 2).

3. Results and Discussion

Figure 1 shows the metallographs of BST thin films etched by various etchants. For the sample etched by pure HF in Fig. 1a, the serious side etching with a zigzag etching edge is observed, and there are some yellow residues. BST films of etching areas can not be removed merely by HNO_3 or H_2O_2 as seen in Fig. 1b and Fig. 1c, and the etching rate is difficult to control. The film showed in Fig. 1d was etched by $HF/HNO_3/H_2O_2/H_2O$ with the volume ratio of 1:25:50:20. The metallograph of BST film exhibits a smooth surface with no residues and the etching edges are clear and have good linearity. In this situation, the etching rate of BST thin film is determined to be about 37 nm/s. Meanwhile, the little distortion is assessed by side etching ratio which is calculated as the absolute of (W-w)/2D. (W represents the designed value of the pattern width, w represents the actual value of the pattern width after etching and D represents the thickness of the BST films.) The designed width is 600 μm and the actual width after etching is 590 μm. So the side etching ratio of BST films is 10:1, which indicates that the distortion is very small using $HF/HNO_3/H_2O_2/H_2O$ etchant.

Figure 2 exhibits the surface morphologies and chemical compositions of BST films before and after etching by SEM with EDS. SEM graph in Fig. 2a shows that the unetched

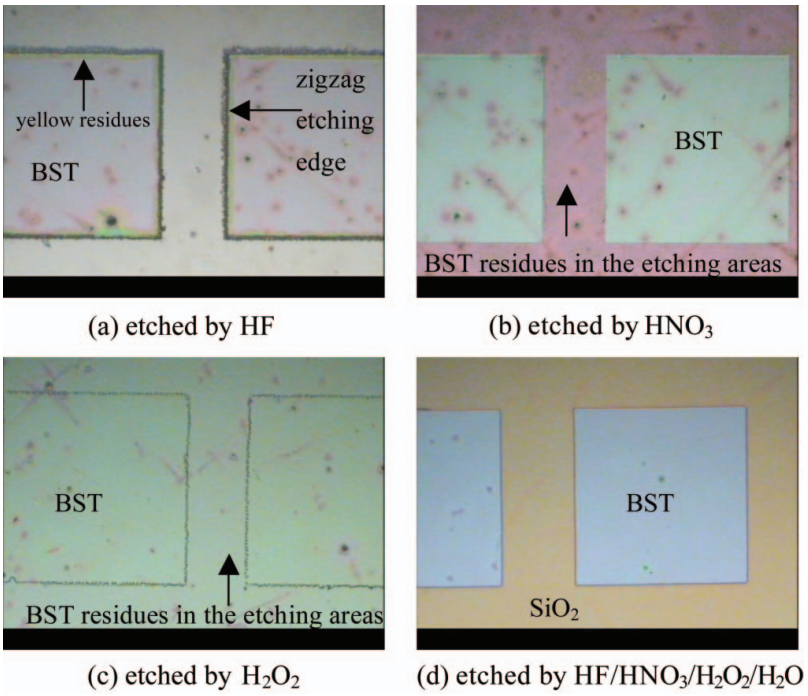

Figure 1. Metallographs of BST thin films etched by different etchant. (See Color Plate XXVII)

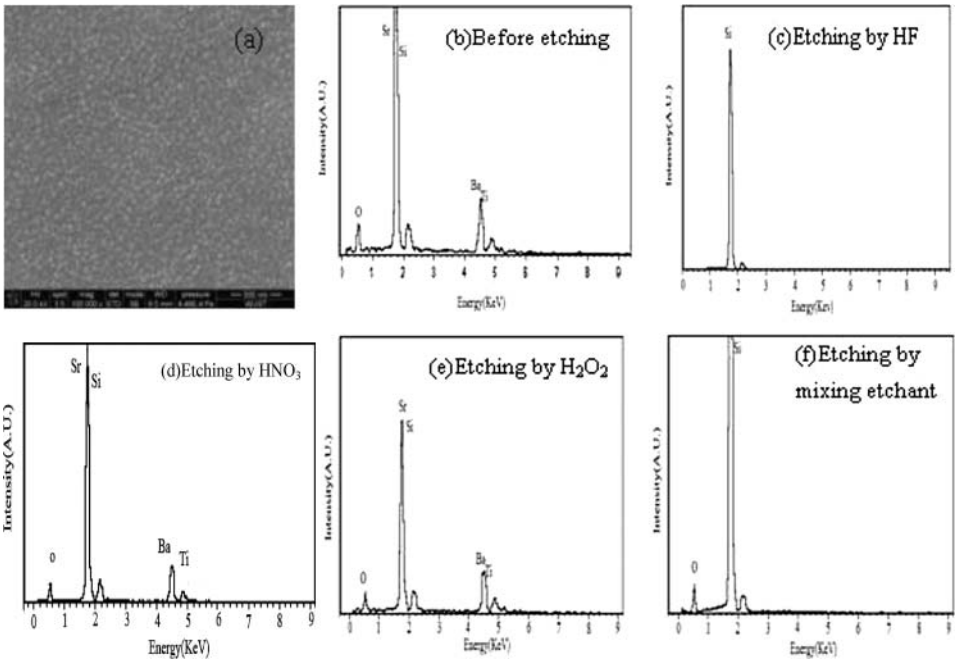

Figure 2. SEM with EDS analysis of BST films annealed at 700°C.

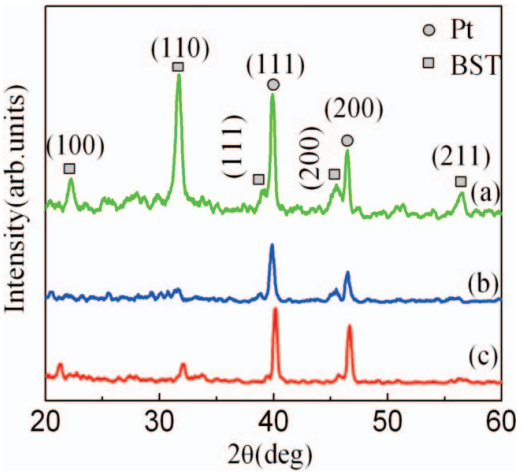

Figure 3. XRD patterns of BST films.

BST thin film is dense, crack-free and pore-free. All the components of BST are detected before etching as shown in Fig. 2b. In Fig. 2c, BST film etched by HF shows that not only BST film is removed but also the SiO_2 layer is etched. As shown in Fig. 2d, the intensities of Ba, Sr and Ti are almost the same as those of the unetched one. It indicates that BST film can not be etched by HNO_3. In Fig. 2e, the intensities of Ba and Sr decrease while the intensity of Ti is just a little weaker. It demonstrates that BST films can not be etched merely by H_2O_2 either. So it is impossible to etch BST films with individual solution of HF, HNO_3 or H_2O_2. The EDS spectra for the BST films etched by two or three solution mixtures of HF, HNO_3 and H_2O_2 were also studied. Compared with these mixtures, etchant with the volume ratio of $HF:HNO_3:H_2O_2:H_2O = 1:25:50:20$ was used successfully for BST thin films etching. Water was added into $HF/HNO_3/H_2O_2$ to obtain a moderate etching rate. Fig. 2f shows that the spectra of Ba, Sr and Ti disappear and only the spectrum of SiO_2 substrate is detected. It indicates that the BST films are removed completely without any residues by the etchant with the volume ratio of $HF:HNO_3:H_2O_2:H_2O = 1:25:50:20$. The chemical reactions during the etching process are as follows:

$$Ba^{2+} + 2F^- \rightarrow BaF_2 \quad (1)$$

$$Sr^{2+} + 2F^- \rightarrow SrF_2 \quad (2)$$

$$Ti^{4+} + 4F^- \rightarrow TiF_4 \quad (3)$$

The results indicate that the reaction rates of Ba, Sr and Ti with the etchants are different. The reactions between Ba^{2+} (Sr^{2+}) and $F^($ are faster than the reaction between Ti^{4+} and F^-–HNO_3 act just as a catalyst for the etching process [12].

Figure 3 illustrates the X-ray diffraction patterns of the unetched, etched and post-annealed BST thin films. In Fig. 3a, the pattern of unetched BST film with peaks corresponding to (100), (110), (111), (200) and (211) indicates a polycrystalline perovskite phase. The XRD pattern of the BST film etched by $HF/HNO_3/H_2O_2/H_2O$ with the volume ratio of 1:25:50:20 is shown in Fig. 3b. A decrease in crystallinity is observed. The peaks of (100) and (211) disappear. Meanwhile, the intensities of (110), (111) and (200) are

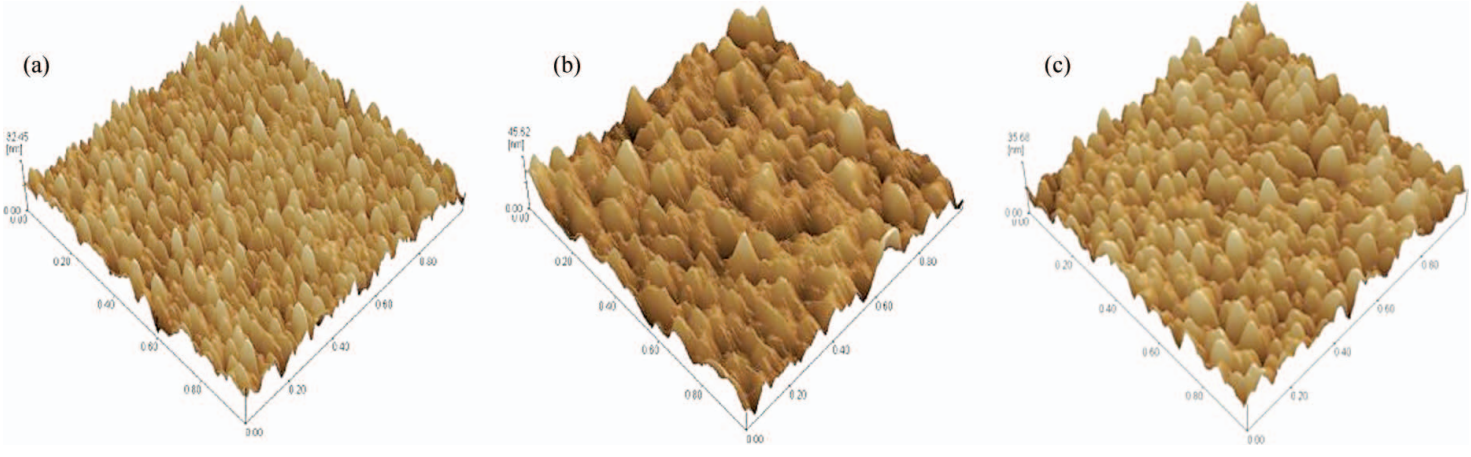

Figure 4. AFM images of BST films. (See Color Plate XXVIII)

[2279/1141

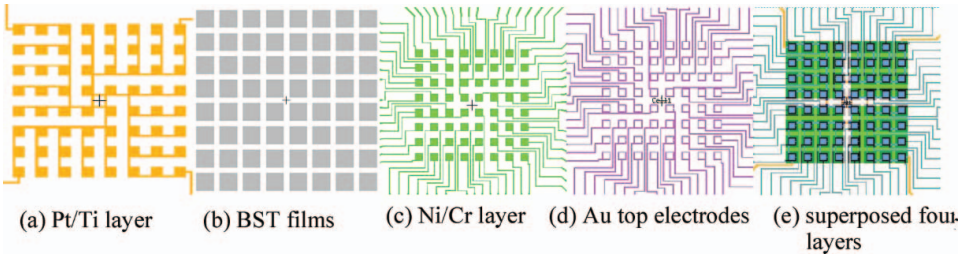

Figure 5. The designed mask patterns of the detector arrays. (See Color Plate XXIX)

much weaker than that of the unetched BST film. This can be explained as follows: the etching by-products such as metal-fluorides and the organic materials after stripping off the photoresist remained on the surface of BST film, which changes the stoichiometry. The deviation of the stoichiometry cause the degradation of crystallinity [13]. As shown in Fig. 3c, even after post-annealing the etched film at 600°C for 30 min, the BST (211) peak do not appear again. The intensities of BST (100) and BST (110) are recovered, which indicates that the residues are removed and the crystallinity of BST thin film is partially recovered.

Figure 4 shows the AFM images of the unetched, etched and post-annealed BST films, respectively. The surface roughness of the films is assessed by root mean square (RMS). In Fig. 4a, the unetched film is fully grown and it presents 3.727 nm in roughness, while the film etched by the etchant of $HF/HNO_3/H_2O_2/H_2O$ with the volume ratio of 1:25:50:20 possesses a RMS of 4.974 nm in Fig. 4b. The reason for increasing in roughness is that the etching reaction often starts at the grain boundary which is a great asylum for deficiencies and impurities. So the depths of pits and holes of etched BST film around the grains become deeper [14]. Furthermore, the different etch rates of (Ba, Sr, Ti) elements result in the nonuniform consumption of the components. However, the RMS of the film by post-annealing with 4.449 nm is larger than that of the unetched film but smaller than that of the etched film in Fig. 4c. It indicates that it is helpful for removing organics and other residues to adjust crystal lattice by thermal treatment.

According to the designing rules of infrared detector, the mask patterns were drawn by L-edit software. Figure 5(a)∼(e) show the mask patterns of the detector arrays of Pt/Ti bottom electrodes, BST films, Ni/Cr absorption layer, Au top electrodes and the superposed four layers of 8 × 8 arrays, respectively. The area of each electrode unit of Pt/Ti and Ni/Cr is 400 × 400 μm^2. The hollow structure of Au top electrodes is designed to make Ni/Cr absorption layer to obtain enough infrared radiation. The BST unit with 600 × 600 μm^2 is made a little larger to prevent the bottom and top electrodes from breakdown. Fig. 6

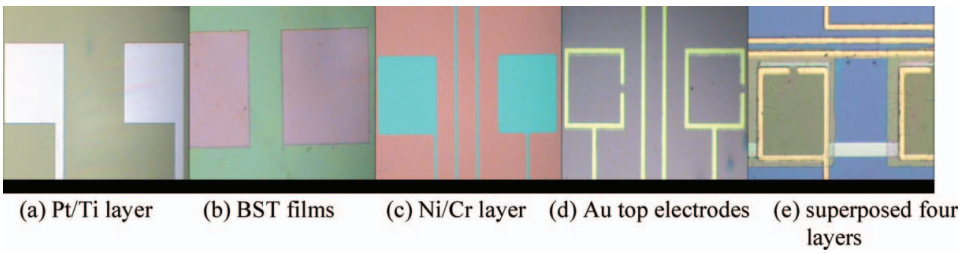

Figure 6. The metallographs of the detector arrays. (See Color Plate XXX)

shows the experimental results of two units in 8 × 8 arrays correspond to Fig. 5. As can be seen from Fig. 6, the surfaces of all films are clean and the edges of the patterns are smooth with very little distortion. It is thus reasonable to expect that the application of Au/Ni/Cr/BST/Pt/Ti infrared detector of 8 × 8 arrays can be realized. Certainly, further study is necessary to ascertain this expectation.

4. Conclusions

Au/Ni/Cr/BST/Pt/Ti infrared detector of 8 × 8 arrays is successfully fabricated. Good electrodes patterns are obtained using lift-off technique. The BST ferroelectric thin films are successfully etched by $HF/HNO_3/H_2O_2/H_2O$ with the volume ratio of 1:25:50:20. The etching rate and the side etching ratio of BST films are about 37 nm/s and 10:1, respectively. The crystallinity and smoothness of the etched BST thin films are recovered by post-annealing. Good electrical properties can be expected by improving the micro-pattern of the thin films and the electrodes.

Acknowledgments

This work has been supported by the National Natural Science Foundation of china through No.50672022 and the Hubei Province Key Laboratory of Refractories and Ceramics Ministry-Province Jointly-Constructed Cultivation Base for State Key Laboratory through No.G0701.

References

1. G. A. Hirata, L. L. López, J. M. Siqueiros, and J. McKittrick, Ferroelectric $Ba_{1-x}Sr_xTiO_3$ thin films for DRAM's applications. *Superficies Vacio.* **9**, 147–149 (1999).
2. S. Chen, H. B. Zhang, S. L. Jiang, Y. K. Zeng, and M. D. Liu, Status and trend of pyroelectric uncooled infrared focal plane arrays. *Infrared and Laser Engineering* **35**, 419–424 (2006).
3. B. S. Zhang, Z. C. Quan, T. J. Zhang, and T. Guo, Effect of oxygen gas and annealing treatment for magnetically enhanced reactive ion etched $Ba_{0.65}Sr_{0.35}TiO_3$ thin flims. *J. Appl. Phys.* **101**, 014107 (2007).
4. D. S. Wuu, F. C. Liao, N. H. Kuo, R. H. Horng, and M. K. Lee, Etching characteristics and mechanism of $Ba_{0.7}Sr_{0.3}TiO_3$ thin films in an inductively coupled plasma. *Jpn. J. Appl. Phys.* **39**, 2068–2072 (2000).
5. P. Shi, X. Yao, and L. Y. Zhang, Reactive ion etching of sol-gel-derived BST thin films. *Ceram. Int.* **30**, 1513–1516 (2004).
6. C. Soyer, E. Cattan, and D. Remiens, Ion beam etching of PZT thin films: Influence of grain size on the damages induced. *J. Eur. Ceram. Soc.* **25**, 2269–2272 (2005).
7. Z. Wang, C. H. Yang, D. L. Sun, J. F. Hu, H. Wang, H. C. Chen, and C. S. Fang, Atomic force microscopic imaging and wet etching of $Bi_2Ti_2O_7$ thin films. *Mater. Sci. Eng. B* **102**, 335–338 (2003).
8. G. H. Kim, K. T. Kim, D. P. Kim, and Chang-Il Kim, Etching characteristic and mechanism of BST thin films using inductively coupled Cl_2/Ar plasma with additive CF_4 gas. *Thin Solid Films* **459**, 127–130 (2004).
9. C. Soyer, E. Cattan, and D. Remiens, Reactive ion beam etching of PZT thin films. *Ferroelectr.* **288**, 253–263 (2003).
10. G. H. Kim, K. T. Kim, D. P. Kim, and Chang-Il Kim, Plasma etching of $(Ba,Sr)TiO_3$ thin films using inductively coupled Cl_2/Ar and BCl_3/Cl_2/Ar plasma. *Thin Solid Films* **475**, 86–90 (2005).
11. J. H. Kim, A. M. Grishin, and V. A. Ignatova, Wet etching study of $La_{0.67}(Sr_{0.5}Ca_{0.5})_{0.33}MnO_3$ films on silicon substrates. *J. Electron. Mater.* **37**, 361–366 (2008).

12. R. T. Zhang, C. R. Yang, A. Yu, B. Wang, H. J. Tang, H. W. Chen, and J. H. Zhang, Wet chemical etching method for BST thin films annealed at high temperature. *Appl. Surf. Sci.* **254**, 6697–6700 (2008).
13. S. K. Choi, D. P. Kim, C. Kim, and E. G. Chang, Damage in etching of (Ba,Sr)TiO_3 thin films using inductively. *J. Vac. Sci. Technol. A* **19**, 1063–1067 (2001).
14. J. Baborowski, P. Muralt, and N. L. edermann, Mechanisms of Pb ($Zr_{0.53}Ti_{0.47}$) O_3 thin film etching with ECR/RF reactor. *Integrated Ferroelectrics* **31**, 261–266 (2001).